Carbohydrate Polymers 153 (2016) 686–695

Contents lists available at ScienceDirect

Carbohydrate Polymers

journal homepage: www.elsevier.com/locate/carbpol

Acetylation of bacterial cellulose catalyzed by citric acid: Use of reaction conditions for tailoring the esterification extent

Jhon Alejandro Ávila Ramírez[a,b], Catalina Gómez Hoyos[c], Silvana Arroyo[d], Patricia Cerrutti[a,e], María Laura Foresti[a,b,*]

[a] Grupo de Biotecnología y Biosíntesis, Instituto de Tecnología en Polímeros y Nanotecnología (ITPN-UBA-CONICET), Facultad de Ingeniería, Universidad de Buenos Aires, Las Heras 2214 (CP 1127AAR), Buenos Aires, Argentina
[b] Consejo Nacional de Investigaciones Científicas y Técnicas (CONICET), Argentina
[c] Facultad de Ingeniería Agroindustrial, Universidad Pontificia Bolivariana, Circular 1° N° 70-01, Medellín, Colombia
[d] Laboratorio de Sólidos Amorfos, Instituto de Tecnologías y Ciencias de la Ingeniería Hilario Fernández Long (INTECIN), Facultad de Ingeniería, Universidad de Buenos Aires, Paseo Colón 850, C1063ACV, Buenos Aires, Argentina
[e] Departamento de Ingeniería Química, Facultad de Ingeniería, Universidad de Buenos Aires, Argentina

ARTICLE INFO

Article history:
Received 17 April 2016
Received in revised form 3 August 2016
Accepted 4 August 2016
Available online 4 August 2016

Keywords:
Bacterial cellulose
Acetylation
Citric acid
Reaction conditions

ABSTRACT

Bacterial cellulose (BC) nanoribbons were partially acetylated by a simple direct solvent-free route catalyzed by citric acid. The assay of reaction conditions within chosen intervals (i.e. esterification time (0.5–7 h), catalyst content (0.08–1.01 mmol/mmol AGU), and temperature (90–140 °C)), illustrated the flexibility of the methodology proposed, with reaction variables which can be conveniently manipulated to acetylate BC to the required degree of substitution (DS) within the 0.20–0.73 interval. Within this DS interval, characterization results indicated a surface-only process in which acetylated bacterial cellulose with tunable DS, preserved fibrous structure and increased hydrophobicity could be easily obtained. The feasibility of reusing the catalyst/excess acylant in view of potential scale-up was also illustrated.

1. Introduction

Cellulose fibers are known to display a hierarchical organization consisting of micrometric-in-length microfibrils composed of amorphous and crystalline domains, with diameter in the ≈2–20 nm range. Individualization of cellulose microfibrils from plant sources requires intensive mechanical treatment, in many cases aided by chemical or enzymatic pretreatments of the lignocellulosic raw materials. Besides, concentrated solutions of strong acids are commonly used to yield the so-called cellulose nanocrystals by selective removal of amorphous domains.

On the other hand, bacterial cellulose (BC) is a quite green alternative for the isolation of pure lignin/hemicellulose-free-cellulose nanoribbons with low energy demand, and no need of harsh chemicals other than diluted aqueous alkali solutions used to remove bacterial cells. Besides chemical purity, bacterial cellulose is also distinguished by its high polymerization degree, high crystallinity, high mechanical strength, and well-separated nano- and microfibrils which create an extensive surface area, and confer BC a high liquid loading capacity.

The mentioned characteristics make BC a remarkably versatile biomaterial with applications in paper products, electronics, acoustic membranes, reinforcement of composite materials, membrane filters, hydraulic fracturing fluids, edible food packaging films, and –due to its unique nanostructure and properties-, in numerous medical and tissue-engineered applications (tissue-engineered constructs, wound healing devices, etc) (Foresti, Cerrutti & Vazquez, 2015). In the widely studied use of BC as nanofiller/reinforcement, however, the OH-rich structure and high hydrophilicity of BC promotes aggregation and hampers its use in most common plastic composites. Chemical modification of cellulose aimed at reducing the number of hydroxyl interactions and increasing its compatibility with several matrices is therefore of great interest. Particularly, the possibility of conferring a hydrophobic character only to the surface of cellulose microfibrils, while keeping the integrity of their crystalline core unchanged, is a challenge that in the last years has triggered much research (Missoum, Belgacem, & Bras, 2013).

To achieve this aim, in the last decade a number of protocols devoted to the esterification (reaction in which hydroxyl

* Corresponding author at: Grupo de Biotecnología y Biosíntesis, Instituto de Tecnología en Polímeros y Nanotecnología (ITPN-UBA-CONICET), Facultad de Ingeniería, Universidad de Buenos Aires, Las Heras 2214 (CP 1127AAR), Buenos Aires, Argentina.
E-mail address: mforesti@fi.uba.ar (M.L. Foresti).

http://dx.doi.org/10.1016/j.carbpol.2016.08.009
0144-8617/

groups are replaced by less hydrophilic ester groups) of never-dried BC pellicles, homogenized BC suspensions, and freeze-dried BC suspensions and pellicles, have been proposed. Among them, methodologies catalyzed by perchloric acid (Gonçalves et al., 2015, 2016; Ifuku et al., 2007; Kim, Nishiyama, & Kuga, 2002; Yamamoto, Horii, & Hirai, 2006), sulphuric acid (Cunha, Zhou, Larsson, & Berglund 2014; Tomé et al., 2011a, 2011b), *p*-toluenesulfonyl chloride (Blaker, Lee, Walters, Drouet, & Bismarck, 2014; Lee & Bismarck, 2012; Lee, Blaker, & Bismarck, 2009; Lee et al., 2011), iodine (Hu, Chen, Xu, & Wang, 2011), pyridine (Agustin, Nakatsubo, & Yano, 2016; Tomé et al., 2010); and α-hydroxy acids such as tartaric, lactic and citric acid (Ávila Ramírez, Gómez Hoyos, Arroyo, Cerrutti, & Foresti, 2016; Ávila Ramírez, Juan Suriano, Cerrutti, & Foresti, 2014) have been reported. Esterification of BC in palmitoyl chloride vapor (Berlioz, Molina-Boisseau, Nishiyama, & Heux, 2009) and in DMAc/LiCl (De Marco Lima, Sierakowski, Faria-Tischer, & Tischer, 2011) has also been proposed.

In reference to the esterification of BC catalyzed by α-hydroxy acids of natural origin, our previous contributions explored the esterification of BC suspensions with acetic and propionic acid catalyzed by L-tartaric acid, as well as the acetylation of BC with acetic anhydride catalyzed by L-tartaric, lactic and citric acids. The acylant was always added in great excess to provide sufficient liquid medium to disperse BC (no extra solvent was incorporated), and the extent of esterification was tuned by adjusting the esterification interval. From the results obtained in the mentioned contributions, it came clear that the α-hydroxy acid with highest activity towards BC acetylation was citric acid. The higher reactivity of acetic anhydride when compared with the corresponding acid was also evidenced (Ávila Ramírez et al., 2014, 2016). So, in the current contribution, the esterification of BC with acetic anhydride using citric acid as catalyst is further explored, but the focus of research is now shifted to the effect of reaction conditions (not only time but also temperature and catalyst content) on the DS conferred to BC. Given the novelty and potentiality of the route, the aim of this study is to gain knowledge on significant variables that would allow tailoring the acetylation degree conferred to BC. The possibility of reusing the catalyst/excess acylant is also of interest for the potential scale up of the route. Characterization in terms of chemical structure, morphology, crystallinity, thermal decomposition and wettability of acetylated BC samples as a function of DS is also provided.

2. Experimental

2.1. Materials

BC production was carried out in static culture using the bacterial strain *Gluconacetobacter xylinus,* NRRL B-42. BC culture medium was formulated using anhydrous dextrose (Biopack), meat peptone (Britania, Laboratorios Britania S.A.), yeast extract (Britania, Laboratorios Britania S.A.), disodium phosphate (Anedra), citric acid (Merck), glycerol (Sintorgan) and corn steep liquor (Ingredion). Acetic anhydride (Merck), citric acid (Merck), hydrochloric acid (Anedra) and sodium hydroxide (Biopack) were all reagent grade chemicals.

2.2. Production of BC

Inocula of *Gluconacetobacter xylinus* NRRL B-42 were cultured in 100 mL Erlenmeyers flasks containing 20 mL of Hestrin and Schramm (HS) medium (Hestrin & Schramm, 1954**)** and incubated under orbital agitation (200 rpm) for 48 h at 28 °C. For BC production, 1% (v/v) inocula were transferred to 10 L steel trays with 5.0 L of fermentation medium containing 4.0% w/v glycerol and 8.0% corn steep liquor, and statically incubated at 28 °C during 14 days. After that time the pellicles were harvested, thoroughly rinsed with distilled water to remove the culture medium, homogenized in a blender in KOH solution (5% w/v) for 5 min, left in alkali at room temperature for 14 h to eliminate the bacterial cells, and finally rinsed with distilled water till neutralization.

2.3. Esterification of BC catalyzed by citric acid

Homogenized BC (0.5 g dry weight, 3.087 mmol AGU (anhydroglucose units)) was solvent exchanged from water through acetic acid into acetic anhydride prior to reaction. Solvent exchange steps implied contacting the BC with 20 mL of acetic acid or acetic anhydride (twice each) for 10 min with stirring followed by vacuum filtration. BC was then contacted with citric acid (0.08–1.01 mmol/mmol AGU) and 50 mL (i.e. 0.53 mol) of acetic anhydride in a 100 mL glass flask equipped with a reflux condenser. The mixture was then heated to the chosen temperature (90–140 °C) under continuous magnetic agitation in a thermostatized oil bath, and acetylation was alternatively run for different reaction intervals (0.5–7 h). Reaction and reaction conditions intervals are schematized in Scheme 1.

Once the chosen reaction time interval was over, the solid product was separated by vacuum filtration and thoroughly washed with distilled water. The filtrate (acetic anhydride in excess + citric acid) was recovered for reuse assays. Reactions were performed in duplicate, being in all cases the error lower than 3%.

The extent of esterification conferred to BC was determined by heterogeneous saponification and back titration with HCl, as detailed elsewhere (Ávila Ramírez et al., 2014**)**. The acyl content and the degree of substitution achieved were then calculated as stated in Eqs. (1) and (2), respectively:

$$\text{Acyl}(\%) = [(V_B - V_S) \times N_{HCl} \times 4,3]/W \quad (1)$$

$$DS = (162 \times \text{Acyl}\%)/[4300 - (42 \times \text{Acyl}\%)] \quad (2)$$

where V_B (mL) is the volume of HCl required for blank titration, V_S (mL) is the volume of HCl required to titrate the sample, N_{HCl} is the normality of the HCl solution, and W (g) is the mass of sample used.

2.4. Characterization of esterified BC

2.4.1. Solid-state CP/MAS ^{13}C nuclear magnetic resonance spectroscopy (CP/MAS ^{13}C NMR)

High-resolution ^{13}C solid-state spectra of grinded samples were collected using the ramp $\{1H\} \rightarrow \{13C\}$ CP/MAS pulse sequence (cross-polarization and magic angle spinning) with proton decoupling. Spectra were collected at room temperature in a Bruker Avance II-300 spectrometer equipped with a 4-mm MAS probe. The operating frequency for protons and carbons was 300.13 and 75.46 MHz, respectively. Glycine was used as an external reference for the ^{13}C spectra and to set the Hartmann-Hahn matching condition in the cross-polarization experiments. According to the sample, the recycling time varied from 5 to 6 s. The contact time during CP was 2 ms. The SPINAL64 sequence (small phase incremental alternation with 64 steps) was used for heteronuclear decoupling during acquisition with a proton field H1H satisfying $\omega 1H/2\pi = YHH1H = 62$ kHz. The spinning rate for all the samples was 10 kHz.

2.4.2. Fourier transform infrared spectroscopy (FTIR)

Fourier transform infrared spectra of native and acetylated grinded BC samples were acquired on an IR Affinity-1 Shimadzu Fourier Transform Infrared Spectrophotometer in absorbance mode. Carefully dried (12.5 mg, 110 °C, 1 h) samples were mixed with previously dried KBr (130 °C, overnight) in the ratio 1:20 and

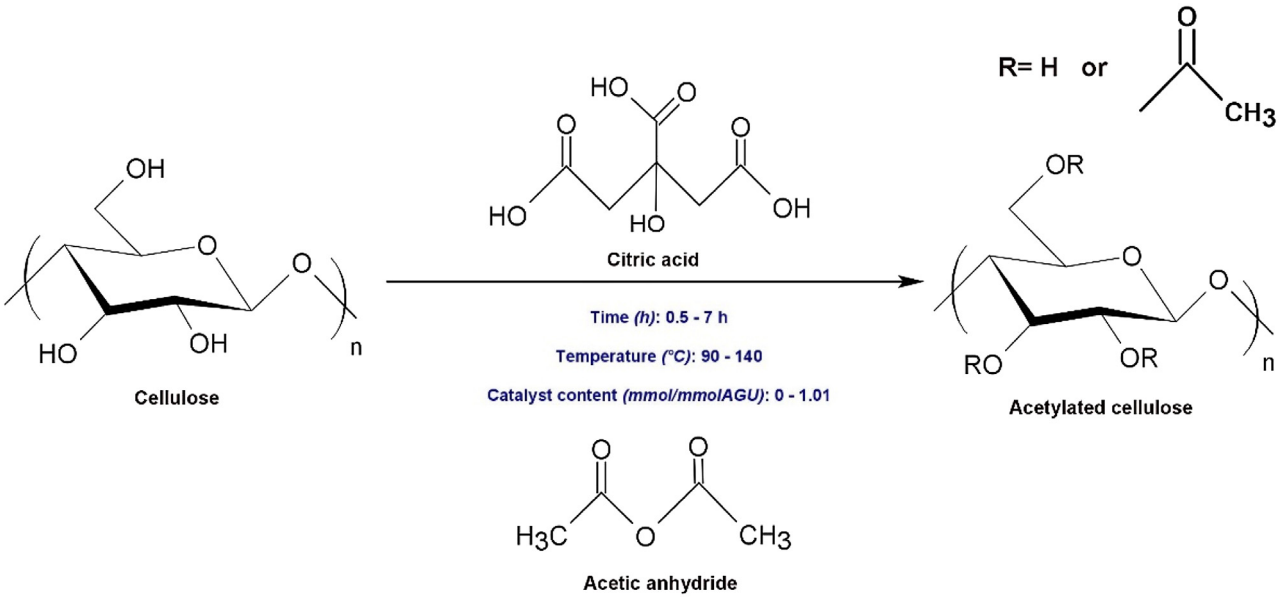

Scheme 1. Acetylation of BC catalyzed by citric acid.

pressed into a disc. Samples were scanned 40 times at a resolution of 4 cm^{-1} in the 4000–700 cm^{-1} range. The derived spectra were baseline corrected and normalized against the intensity of the absorption at 1165 cm^{-1}, corresponding to the (C—O—C) link of cellulose (Ilharco, Gracia, da Silva, & Ferreira, 1997; Lee et al., 2011).

2.4.3. Field emission scanning electron microscopy (FESEM)

One drop of 0.2% native and acetylated BC suspension in water was placed in microscope glasses to be attached to the samples holder, allowed to dry at 100 °C for 5 min, sputter-coated with gold, and observed in a scanning electron microscope Zeiss Supra 40 with field emission at an accelerating voltage of 3 kV.

2.4.4. X-ray diffraction (XRD)

Grinded samples of native and acetylated BC were irradiated with Cu/Kα (k = 0.154 nm) radiation in Rigaku D/Max-C Wide Angle automated X-ray diffractometer with vertical goniometer, operating at 40 kV and 30 mA. This diffractometer has a goniometer design that satisfies the Bragg-Bentano's focusing conditions and it has a curved single crystal (GRAPHITE) monochromator. The slits used were: 1.0 DS (divergence slit) – 1.0 SS (scattering slit)- 0.6 mm-0.8 mm. The X-ray diffraction pattern was recorded in a 2θ angle range of 10–45° at a scan rate of 0.6°/min with a step size of 0.02°. The crystallinity index was determined from the normalized diffraction profiles using Segal's equation (Segal, Creely, Martin, & Conrad, 1959):

$$CrI = (I_{002} - I_{am})/I_{002} \times 100 \quad (3)$$

where I_{002} corresponds to the maximum intensity of the 002 lattice diffraction, and I_{am} is the intensity at 2θ = 18°, after the subtraction of the background signal measured without BC.

2.4.5. Thermogravimetric analysis (TGA)

Thermogravimetric analysis of dried grinded samples (2.5–3 mg, 110 °C, 2 h) was conducted in a TGA-50 Shimadzu instrument. Temperature programs were run from 25 °C to 550 °C at a heating rate of 10 °C/min, under nitrogen atmosphere (30 mL/min) in order to prevent thermoxidative degradation. The initial moisture content of the samples ranged between 5 and 7%.

2.4.6. Contact angle measurements

Native and acetylated BC samples were made into films (1.5–2 cm width, 10–13 cm length) by spreading and drying the recovered nanofibrils suspension (200 mg dried weight) between nylon-covered microscope glasses at 110 °C for 30 min. Immediately before analysis membranes were further dried at 105 °C for 12 h. Equilibrium contact angles of native and acetylated BC pellicles were measured using a contact angle goniometer (OCA 15LHT Plus photo-microscope, Dataphysics). For each film five sessile contact angles were registered at room temperature during 180 s after deposition of 50 μL distilled water drops, and an arithmetic mean of the equilibrium contact angle was calculated. Images of the sessile drops were processed using SCA20 software.

3. Results and discussion

3.1. Citric acid-catalyzed acetylation of BC: effect of reaction conditions

Although their catalytic mechanism has not been completely elucidated, esterifications catalyzed by α-hydroxy acids have been proposed to proceed via a nucleophilic attack of the acylant by the hydroxyl groups of the α-hydroxy acid, followed by second nucleophilic attack of the intermediate formed by the hydroxyl groups of cellulose (Domínguez de María, 2010; Hafrén & Córdova, 2005). Among other α – hydroxy acids assayed, previous results of our group dealing with the esterification of bacterial cellulose nanoribbons (using acetic anhydride as acylant and in absence of added cosolvents), have illustrated the higher catalytic activity of citric acid. At definite reaction conditions (0.5 g BC dry weight – 3.087 mmol AGU, 0.53 mol of acetic anhydride, 3.1 mmol citric acid, 120 °C), the sole manipulation of reaction time allowed obtaining acetylated BC with DS in the 0.27–0.90 interval (Ávila Ramírez et al., 2016). Aiming to gain further knowledge on the system variables and how they can be manipulated in order to tailor the acetylation extent of BC, and working with much lower catalysts amounts, the effect of reaction conditions on the DS conferred to BC is herein assayed (Fig. 1).

Fig. 1a illustrates the effect of reaction time on the DS conferred to BC when the catalyst content (defined as the ratio of catalyst mmol to AGU mmol) was fixed at 0.34 mmol/mmol AGU,

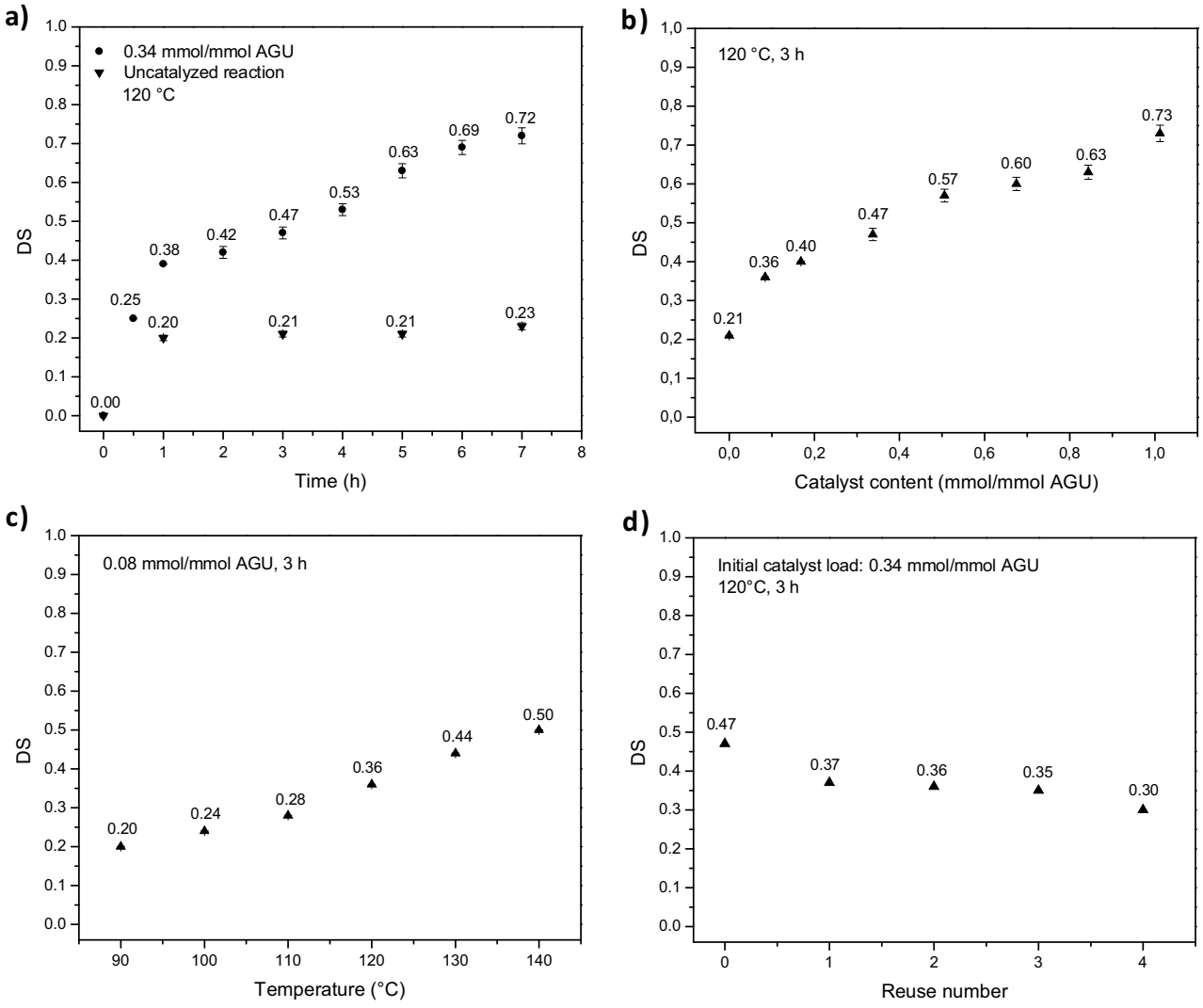

Fig. 1. Effect of reaction variables on the DS conferred to BC. a) effect of reaction time, 0.34 mmol citric acid/mmol AGU, 120 °C; b) effect of citric acid content, 120 °C, 3 h; c) effect of reaction temperature, 0.08 mmol citric acid/mmol AGU, 3 h; d) Catalyst reuse, initial catalyst content: 0.34 mmol citric acid/mmol AGU, 120 °C, 3 h.

and temperature was set at 120 °C. As it is shown, under the chosen conditions, varying the reaction interval from 30 min to 7 h allows tuning the DS of bacterial cellulose nanoribbons in the 0.25–0.72 interval. On the other hand, within the time interval analyzed, the uncatalyzed reaction allowed a maximum DS of 0.23 (7 h). Further assays were carried out during a fixed intermediate reaction interval of 3 h.

Fig. 1b shows the effect of catalyst content (mmol catalyst/mmol AGU) on the DS attained in the acetylation of BC carried out at 120 °C during 3 h. As it is illustrated catalyst content has also a great impact on the acetylation level achieved, with DS values that increase with catalyst content (0.00–1.02 mmol/mmol AGU) in the 0.21–0.73 range. The DS value of 0.21 corresponds to the uncatalyzed reaction. Aiming to minimize catalyst content, in further assays citric acid was kept at 0.08 mmol/mmol AGU.

Fig. 1c summarizes the effect of reaction temperature on the DS conferred to BC after 3 h of reaction using a constant catalyst content of 0.08 mmol/mmol AGU. As it is illustrated, the increase of reaction temperature from 90 to 140 °C continuously enhanced the acetylation level achieved, reaching a DS of 0.50 for the reaction carried out at 140 °C.

From Fig. 1a–c it results that the citric acid-catalyzed route herein proposed is sufficiently flexible to allow tuning the DS conferred to BC in the ≈0.2–0.7 interval by conveniently manipulating time, catalyst content and/or temperature; according to the process possibilities and associated costs. As it will be further discussed, this DS interval is of particular interest since it has generally led to surface-only esterification of BC (Ávila Ramírez et al., 2014, 2016; Agustin et al., 2016; Ifuku et al., 2007; Kim et al., 2002).

Previous reports on bacterial cellulose acetylation by alternative methodologies have generally controlled DS by manipulating mainly reaction time (Hu et al., 2011; Suetsugu, Kotera, & Nishino, 2009; Yamamoto et al., 2006) and the amount of the acetylation reagent used (Ifuku et al., 2007; Kim et al., 2002), with positive correlations in both cases. Positive effects on DS of reaction temperature and catalyst content have also been reported by Hu et al. (2011) for the solvent-free acetylation of BC using iodine as catalyst. Temperature effects were explained in terms of the increased swelling ability of cellulose and diffusion rate of acetic anhydride/catalyst; whereas catalyst content effects were attributed to more acetic anhydride–catalyst intermediates present at higher catalyst concentrations.

Although not particularly expensive, the possibility of reusing the catalyst and the unreacted acylant is always of interest, especially when scale-up is envisaged. The reaction system herein proposed is a heterogeneous one in which BC is kept in suspen-

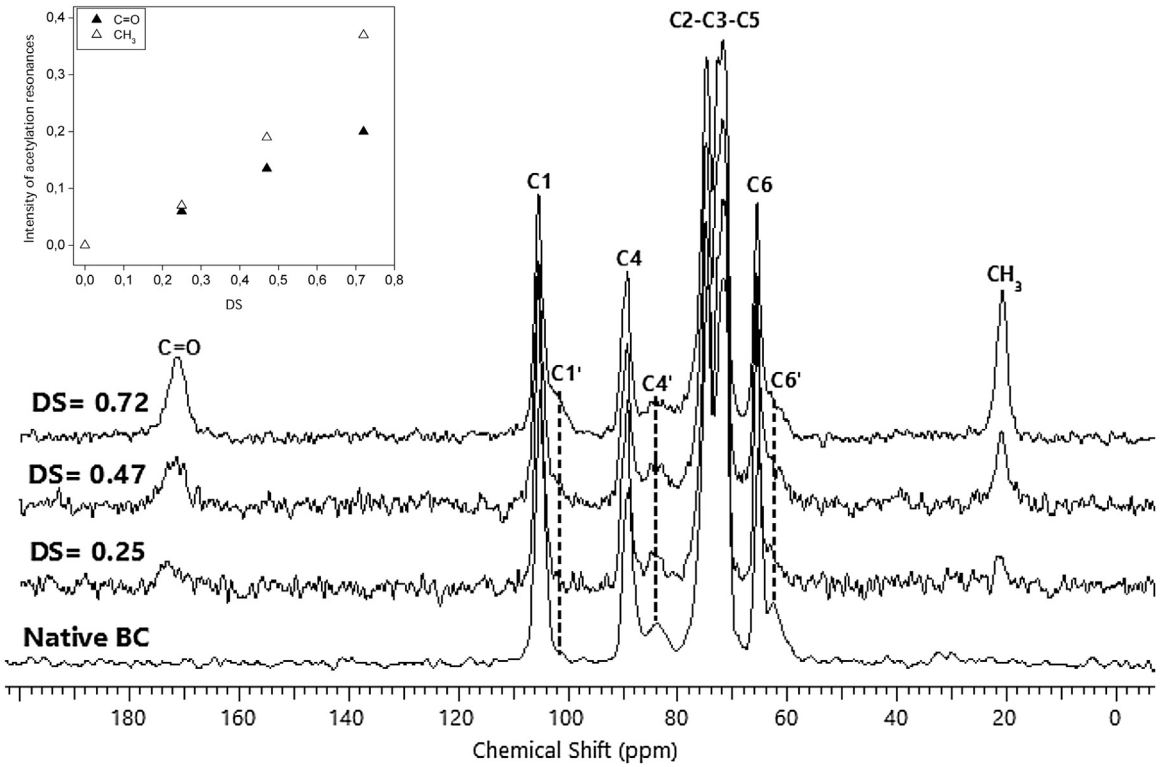

Fig. 2. Solid-state CP/MAS ^{13}C NMR spectra of native and acetylated BC. Inset: Intensity of C=O and CH_3 lines versus DS.

Table 1
Importance of proper solvent exchange of BC prior to reaction. DS attained under definite acetylation conditions (0.34 mmol citric acid/mmol AGU, 120 °C, 3 h) upon different solvent exchange protocols applied to BC suspension.

Solvent exchange protocol applied to BC	DS
From water through acetic acid into acetic anhydride, twice, 20 mL each time.	0.47
From water into acetic acid, twice, 20 mL each time.	0.19
No solvent exchange	0.06

sion and citric acid is dissolved in an excess of acetic anhydride. Since no additional solvent is added, at the end of the reaction the derivatized BC might be removed by filtration/centrifugation and the unreacted acetic anhydride with the dissolved catalyst may be reused. Although in each reuse a fraction of acylant (and dissolved catalyst) would be lost during recovery operations, in the reuse assays herein performed BC was vacuum filtrated and squeezed to reduce this fraction to 1–2% v/v. This volume was replaced with fresh acylant (0.5–1 mL) after each batch. Fig. 1d summarizes the DS values attained after several reuses of the catalyst for an initial citric acid content of 0.34 mmol/mmol AGU (120 °C, 3 h, DS = 0.47 according to Fig. 1a).

As it is shown in Fig. 1d, under these conditions up to three reuses of the catalyst/acylant are possible with a reduction of DS of 25% (DS is reduced from 0.47 to 0.35) for a remaining catalyst content of ≈95% (a catalyst loss proportional to the acylant fraction lost was assumed). The reasons for the observed reduction in acetylation extent with catalyst/acylant reuse are currently under study. The effect of acetic acid produced during reaction, which may further react to produce water later involved in acetic anhydride hydrolysis is one possibility. The detrimental effect of the presence of acetic acid and/or water in the reaction medium is also illustrated by the effect on DS of the initial solvent exchange protocol applied to BC (Table 1). On the other hand, loss of citric acid due to cross-linking reactions can be ruled out from CP/MAS ^{13}C NMR data (please refer to Fig. 2), in which no signal attributed to citric acid is observed.

3.2. Characterization of acetylated BC with varying DS

Results included in the previous section demonstrated how reaction conditions (time, catalyst content, reaction temperature) may be conveniently manipulated to modulate the derivatization extent conferred to BC in the 0.20–0.73 interval. In the current section, acetylated BC samples with varying DS within that interval are characterized by means of Solid-state ^{13}C NMR, FTIR, FESEM, XRD, TGA, and water contact angle. Representative samples chosen for characterization are those resulting from the effect of time on DS (Fig. 1a).

3.2.1. Solid-state CP/MAS ^{13}C NMR spectroscopy

Fig. 2 shows the solid state CP/MAS ^{13}C NMR spectra obtained for native and chosen acetylated BC samples. Native BC spectrum showed carbon resonances typical of cellulose I, i.e. C1: 105.1 ppm, C4: 89.1 ppm, C4′: 84.1 ppm, cluster C2-C3-C5: 80–69 ppm, C6: 65.3 ppm, and C6′: 62.7 ppm. On the other hand, CP/MAS ^{13}C NMR of acetylated BC samples gave evidence of the success of citric acid-catalyzed acetylation, by appearance of two new resonances centered at 21 ppm and 171–173 ppm, which were attributed to the carbons involved in CH_3 and C=O of the acetate groups, respectively (Table 2). The intensity of these resonances increased with the extent of acetylation (Fig. 2, inset). With acetylation also a small shoulder at 102 ppm became visible, assignable to C1′ resonance line. The onset with esterification of this new contribution assigned to C1′ has been reported previously for BC, tunicin whiskers and highly bleached sulfite cellulose fibers (Berlioz et al., 2009; Jandura, Kokta, & Riedl, 2000). On the other hand, the absence of resonances at ≈44 ppm indicates that samples are free of citric acid acting as

Table 2
Ppm assignment of CP/MAS ^{13}C NMR solid state spectra of native and acetylated BC. For de C2-C3-C5 cluster the ppm interval is given.

Sample	C=O	C1	C1′	C4	C4′	Cluster C2-C3-C5	C6	C6′	CH_3
Native BC	–	105.1	102.2	89.1	84.1	79.7–68.5	65.3	62.7	–
DS = 0.25	173.1	105.5	102.2	89.3	84.3	79.7–69.3	65.6	63.3	21.2
DS = 0.47	171.5	105.4	101.4	89.3	84.0	79.6–69.3	65.7	61.8	21.0
DS = 0.72	171.0	105.4	101.4	89.2	83.8	79.5–68.5	65.6	61.2	20.8

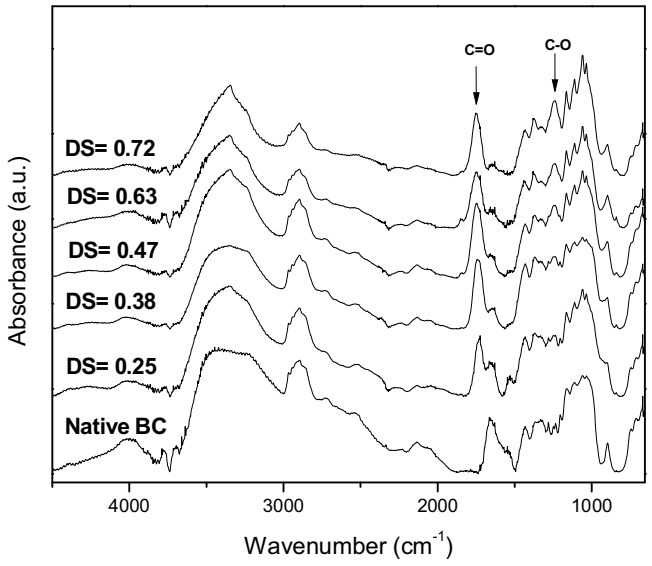

Fig. 3. FTIR spectra of native and acetylated BC.

cross-linker, esterified citric acid or free citric acid simply remaining after product recovery.

3.2.2. FTIR spectroscopy

Fig. 3 collects the FTIR spectra of native and acetylated BC. The peaks centered at 3345, 2895, 1432, 1278, 1165, 1109, 1059, and 897 cm^{-1} are typical of native cellulose (Castro et al., 2011; Ilharco et al., 1997). In accordance with ^{13}C NMR data, upon acetylation three new bands assignable to the acetyl groups introduced appeared in the spectra confirming esterification: i.e. 1745 cm^{-1} corresponding to the ester C=O stretching mode, 1371 cm^{-1} attributed to C—H bending, and 1243 cm^{-1} assignable to the C—O stretching vibration of the acetate groups. Moreover, upon acetylation the intensity of the absorbances associated with the vibration of OH groups (≈3300 cm^{-1}) and –more noticeably- the H—O—H bending vibration of absorbed water molecules (1645 cm^{-1}) were reduced.

3.2.3. Field emission scanning electron microscopy

Fig. 4a–f display the FESEM micrographs of neat and acetylated BC samples obtained by variation of the esterification interval (samples from Fig. 1a, DS 0.25–0.72). Neat BC shows 30–40 nm-width micrometric-in-length interwined ribbons. The ribbon-like morphology of BC nanofibers with rectangular cross-section typical of *Acetobacter* microfibrils, as well as their tendency to twist and kink is highlighted by arrows included in Fig. 4a.

As it is shown in Fig. 4b–h, irrespectively of their DS, the morphology of the acetylated BC ribbons remained similar to that of control samples, with no significant change in nanoribbons width (e.g. average width of native BC out of 40 measurements: 33 ± 3 nm, average width of acetylated BC with DS = 0.72 (40 measurements): 33 ± 2 nm); no visible damage on the fibrils surface; and with the rectangular cross-section (arrows in Fig. 4e) and web-like fibrous structure typical of bacterial cellulose being preserved.

Figs. 4g (DS = 0.50) and 4h (DS = 0.73), correspond to acetylated samples with similar DS than those shown in Fig. 4d (DS = 0.47) and f (DS = 0.72), respectively; although conditions used to obtain them were rather different. For example, Fig. 4g corresponds to the sample acetylated at 140 °C (highest temperature assayed in Fig. 1c). As it is shown, no evidence of nanoribbons deterioration at this reaction temperature is observed. By the way, comparison of Fig. 4f and h demonstrated that extended reaction time did not promote any significant change in samples morphology.

3.2.4. X-ray diffraction analysis

The X-ray diffraction profiles of native and acetylated BC with increasing DS are presented in Fig. 5a. BC has a typical cellulose I structure with three well-defined diffraction peaks centered at 2θ = 14.4° (101), 16.7° ($10\bar{1}$) and 22.6° (002) which confirmed that only cellulose I was present in all samples (Johnson Ford, Mendon, Thames, & Rawlins, 2010). After acetylation, the XRD profiles of esterified BC still showed the same distinct peaks as neat BC, together with two very small peaks centered at 20.3° (021) and 34.6° (040) which became visible. These diffraction peaks are also characteristic of Cellulose I and have previously been observed for neat BC by other authors with varying relative intensity depending on the BC source and incubation time used (Cerrutti et al., 2016; Ifuku et al., 2007; Kim et al., 2002).

In quantitative terms, crystallinity index (CI) values determined by use of Segal equation after baseline subtraction of the spectrum, indicated no significant reduction in samples crystallinity up to a DS of 0.47. For those samples the relative reduction in CI compared with neat BC was 3%. On the other hand, samples with the highest DS values herein attained (0.63 and 0.72) showed a maximum CI loss of 6% with respect to that of neat BC (taken as 100%). The previous evolution of CI with acetylation extent suggests that the citric acid-catalyzed acetylation of BC up to a DS of 0.72 involved mainly the OH groups on the surface or in the disordered domains of BC, not significantly affecting its ultrastructure (Lee et al., 2011; Tomé et al., 2011b).

The previous is in line with XRD results of acetylated BC with similar DS obtained by other derivatization protocols. For example, Agustin et al. (2016) indicated that pyridine-catalyzed acetylation of BC in *N*-methyl-2-pyrrolidone up to a DS of 0.38 did not affect the crystalline core of the nanocellulose. Besides, in the pioneer contribution of Kim et al. (2002) devoted to BC acetylation catalyzed by perchloric acid in acetic acid/toluene/acetic anhydride medium, authors observed that the X-ray diffraction from cellulose I remained nearly the same up to DS 0.37. On the other hand, the sample esterified up to a DS of 2.77 gave a well-defined pattern of cellulose triacetate, showing strong peaks at 2θ = 7.5° and 26°. Accordingly, with the same acetylation protocole, Ifuku et al. (2007) indicated that the diffraction pattern of acetylated BC with DS = 0.45 almost agreed with that of the untreated sample, whereas samples with DS 0.95 and 1.55 had smaller diffraction peaks from cellulose and gave a well-defined pattern of cellulose triacetate at 2θ = 26° and an amorphous halo. In both contributions, authors concluded that acetylation proceeded highly inhomogeneously, i.e. progressively from the surface to the core of bacterial cellulose nanofibers (Ifuku et al., 2007; Kim et al., 2002). Furthermore, in the solid-phase acetylation of bacterial cellulose Yamamoto et al. (2006)

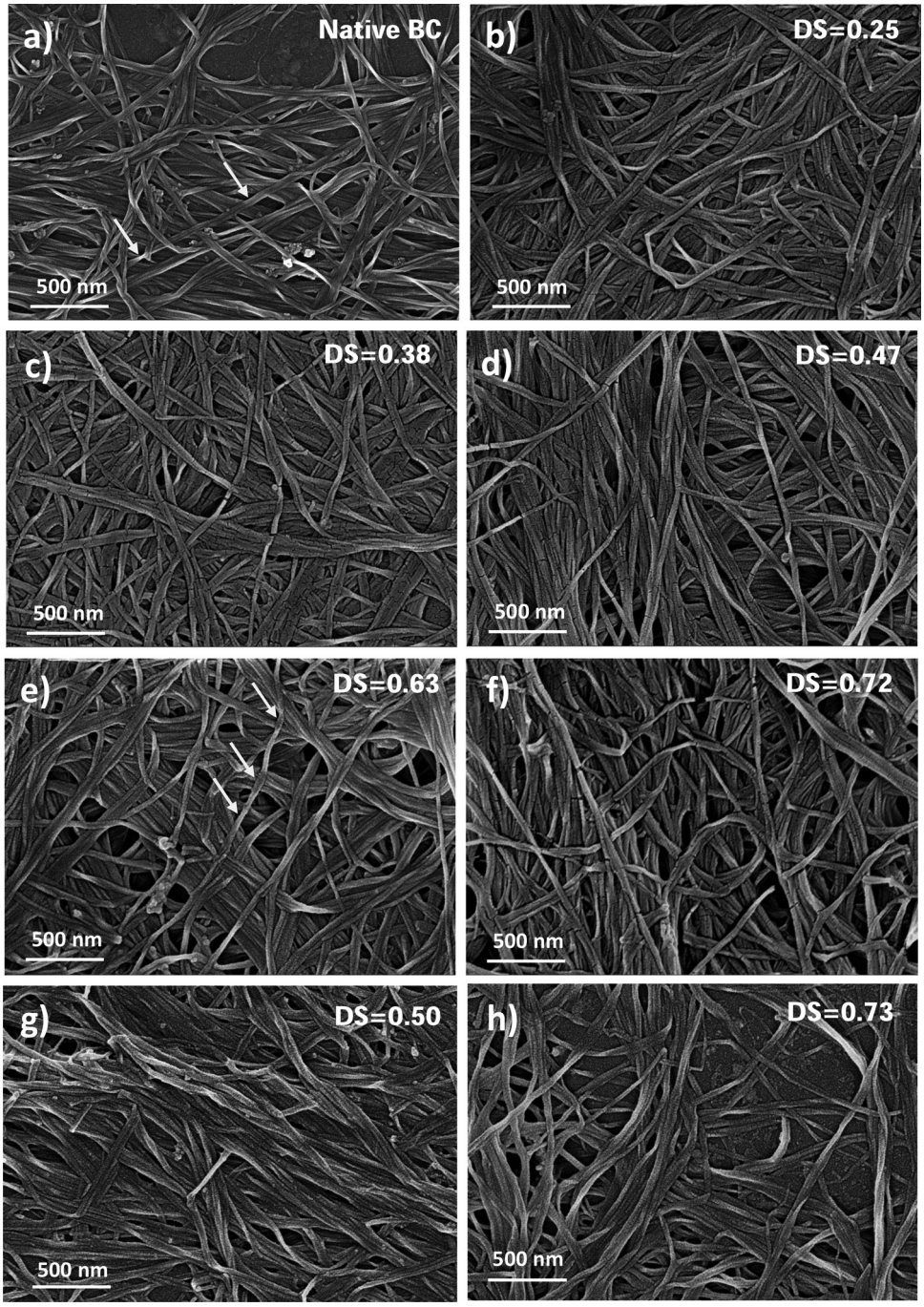

Fig. 4. Field emission scanning electron micrographs of (a) native and (b–h) acetylated BC, 3 KV, 100.000X. (b–f) Samples resulting from the assay of reaction time in Fig. 1a, 0.34 mmol citric acid/mmol AGU, 120 °C. (g) Acetylated BC sample obtained at the highest temperature assayed in Fig. 1c, i.e. 140 °C, 0.08 mmol citric acid/mmol AGU, 3 h. (h) Acetylated BC sample obtained with the highest citric acid content used in Fig. 1b, i.e. 1.02 mmol/mmol AGU, 120 °C, 3 h. Arrows highlight the rectangular cross-section and the tendency to twist and kink of BC microfibrils.

commented on the appearance of broad reflections at $2\theta \approx 8^\circ, \approx 17^\circ$ and $\approx 22^\circ$ for DS ≥ 1 assignable to cellulose triacetate I crystals. The slight but progressive increase with DS of the intensity of the peak centered at 16.7° herein observed (especially when compared with the intensity of the peak at 14.7°) may suggest some contribution of cellulose triacetate I crystals ($2\theta = 17^\circ$), specially for the highest DS values achieved. Similar results have previously been observed by other authors dealing with BC acetylation (Hu et al., 2011; Lee & Bismarck, 2012; Lee et al., 2011).

In terms of the effect of reaction conditions used to attain a definite DS, XRD data from the sample with DS = 0.50 acetylated during 3 h at 140 °C, as well as XRD data from the sample with DS = 0.73 produced in 3 h but using higher catalyst contents, indicated no visible change in the diffractograms with respect to those obtained at lower temperature, or by using lower catalyst content but longer esterification intervals (Fig. 5b).

3.2.5. Thermogravimetric analysis

The impact of acetylation on the thermal stability of BC was evaluated by thermogravimetry. Fig. 6a shows TG data whereas Fig. 6b collects the results obtained in terms of the first derivative of TG signals (DTG) normalized with respect to the initial sample

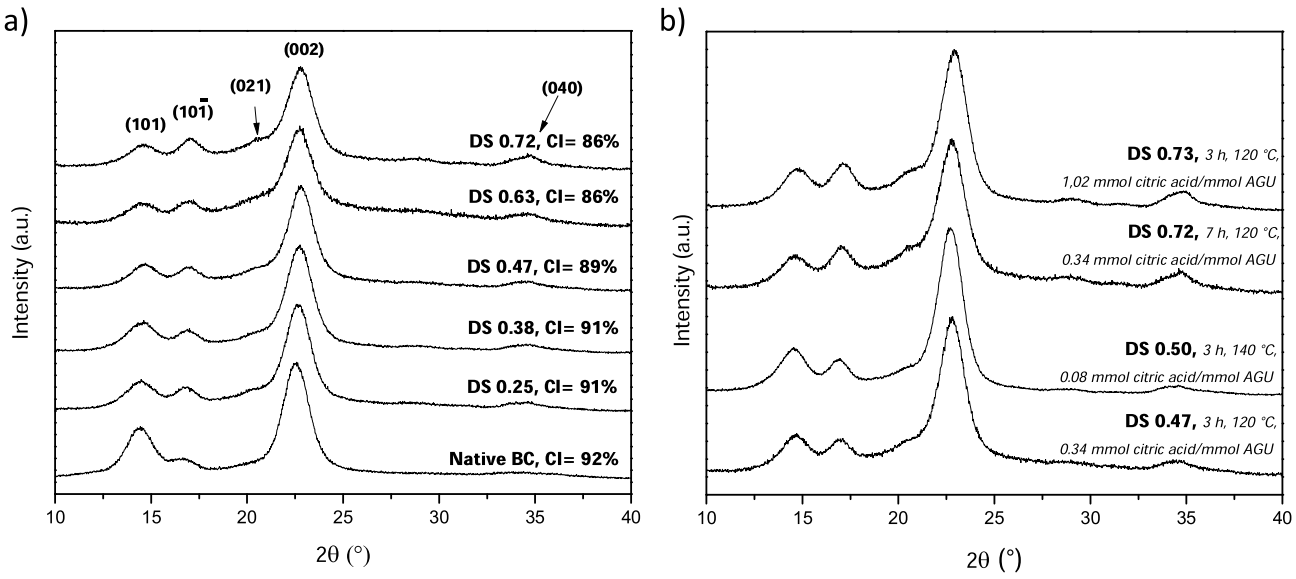

Fig. 5. (a) X-ray diffraction data from native and acetylated BC. (b) X-ray diffractograms of samples with similar DS attained using different reaction conditions.

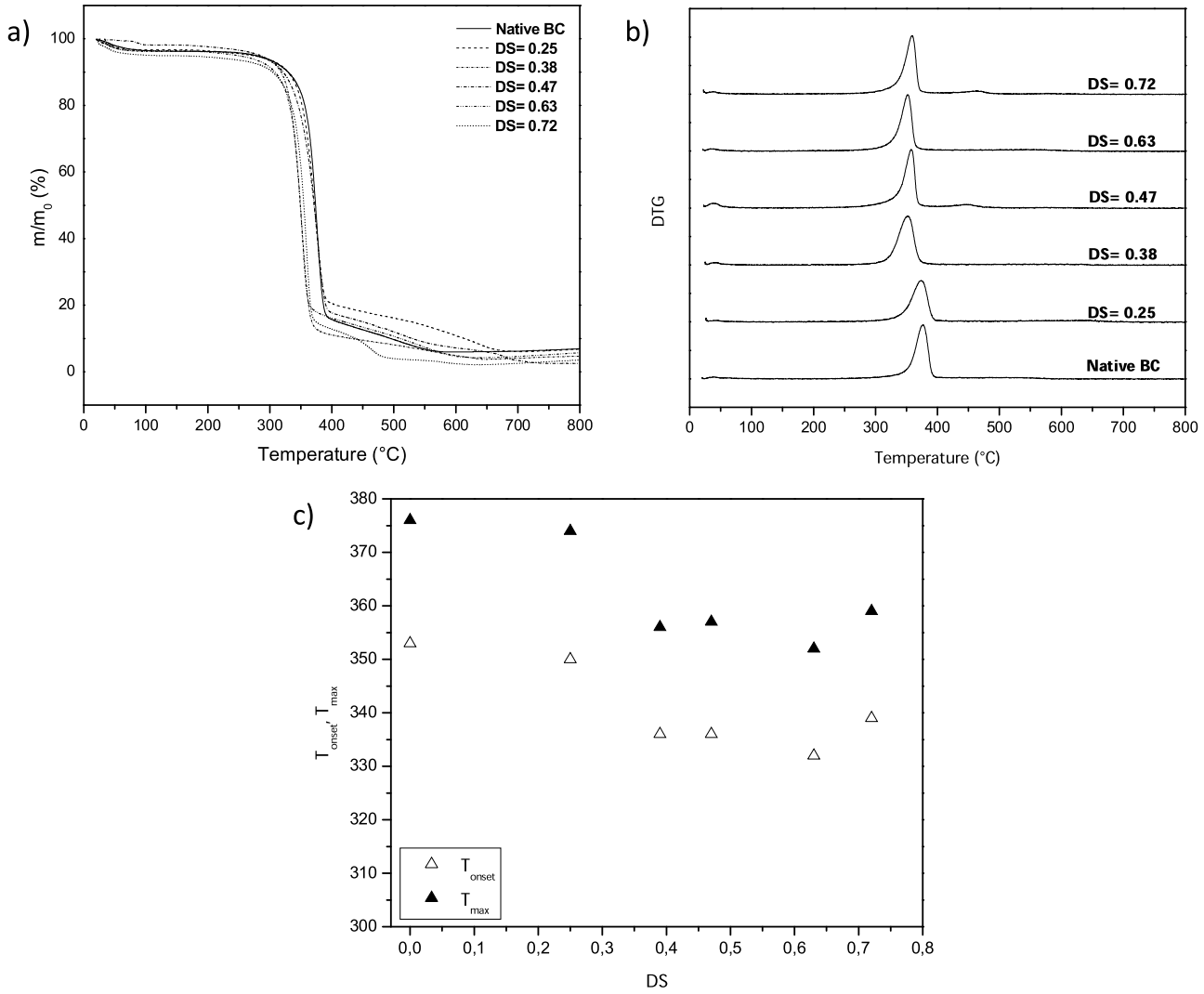

Fig. 6. TG (a) and DTG (b) data from native and acetylated BC. DTG data have been moved in the y-axes for clarity purposes. (c) Evolution of T_{onset} and T_{max} as a function of DS.

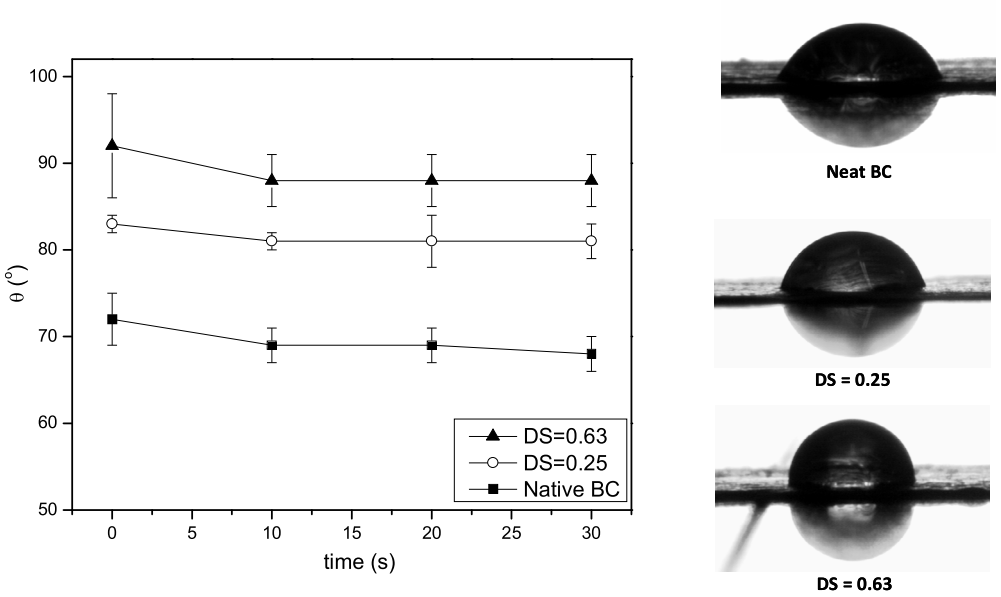

Fig. 7. Evolution of contact angles for native and acetylated BC (DS = 0.25 and DS = 0.63). Images of water drops used to determine equilibrium contact angles, 30 s.

mass. Both, native and esterified BC showed two weight losses (i.e. two peaks in DTG data), attributed to samples dehydration (small weight loss observed between room temperature and ≈ 130 °C) and single-step sample decomposition which for all samples occurred in the ≈ 300–400 °C interval. Since samples have been preconditioned at 110 °C during 2 h, moisture removed in the first weight loss was in all cases between 3 and 5%.

Fig. 6c summarizes the evolution with DS of the corresponding T_{onset} (calculated as the intersection of the extrapolated pre-decomposition ordinate value and a tangential line drawn to the point of steepest slope of the weight loss curve in the decomposition region), and T_{max} (temperature of maximum weight loss rate). As it is shown, when BC was acetylated up to a DS of 0.25, the characteristic T_{onset} and T_{max} of neat BC (353 °C and 376 °C, respectively) were highly preserved, with only 2–3 °C reduction. On the other hand, for higher acetylation levels, the corresponding T_{onset} and T_{max} values were ≈15–20 °C lower than those determined for neat BC. This slight decrease in thermal stability has previously been found in surface-acetylated cellulose fibers and nanofibers (Freire, Silvestre, Neto, Belgacem, & Gandini, 2006; Freire, Silvestre, Neto, Gandini, Martin, & Mondragon, 2008; Tomé et al., 2011a). In accordance with the results from XRD, the still relatively close decomposition temperatures of neat and acetylated BC further indicated that the chemical modification did not destroy the crystalline structure of the original BC nanoribbons. Reduced thermal stability of nanocellulose upon esterification has been frequently explained in terms of reduced crystallinity (not observed by the current route), high liability of the ester linkages introduced, and/or reduced number of effective hydrogen bonds remaining among BC nanofibers upon esterification (Tomé et al., 2010, 2011b; Uschanov, Johansson, Maunu, & Laine, 2011; Lee et al., 2011).

3.2.6. Water contact angles

Contact angles between BC pellicles and water were determined aiming to evaluate the effect of acetylation on the hydrophilicity of the samples.

The evolution of contact angles with time for neat and acetylated BC (DS = 0.25 and DS = 0.63) is shown in Fig. 7. From these data measurement at 30 s was chosen for determination of equilibrium contact angles, and the corresponding water drops images were included in Fig. 7. Contact angles determination illustrated the hydrophobization induced by the modification proposed, with values that increase from 68° ± 2° (neat BC) to 81° ± 2° and 88° ± 3°, for DS = 0.25 and DS = 0.63, respectively. Evidently, the OH rich neat BC surface was more capable of establishing hydrogen bonds with water than acetylated BC samples, consequently resulting in a smaller contact angle value. The reduction in the hydrophilicity of BC is expected to potentially improve its dispersion and interfacial adhesion in nonpolar polymeric matrices, ultimately improving the performance of the resulting nanocomposites.

4. Conclusion

Triggered by previous results of the group evidencing the potential of the citric-acid catalyzed acetylation of bacterial cellulose nanoribbons in solvent-free medium under fixed reaction conditions, the current contribution focused on gaining knowledge on how process variables could be manipulated to provide BC with a definite acetylation extent. Results herein obtained evidenced the flexibility of the methodology proposed, in which reaction time, catalyst content and temperature all showed to be proper variables for tailoring the acetylation extent conferred to BC within the ≈ 0.2–0.7 DS range. The analysis performed also allowed using much lower catalyst contents than previous reports by the current route and, in any case, the feasibility of catalyst/excess acylant reuse was demonstrated for the first time.

Characterization results confirmed hydrophobization and indicated the smooth character of the esterification route proposed, which promoted a relatively low reduction in the crystallinity and the thermal stability of BC, even for the highest DS obtained. Besides, SEM images evidenced the conservation of the fibrillar structure of bacterial cellulose nanoribbons; all suggesting that reaction occurred predominantly on their outmost and amorphous regions without affecting in a great extent the internal structure of the nanoribbons. Initial characterization data also suggested that using higher reaction temperatures or longer time intervals for attaining a certain DS, had no significant effect on acetylated BC properties. The previous results further highlight the importance of the parametric analysis performed for widening the possibilities of controlling the substitution degree conferred to BC by manipulating the most convenient/cost-effective reaction variable.

Conflict of interest

The authors confirm that this article content has no conflict of interest.

Acknowledgements

Authors acknowledge Consejo Nacional de Investigaciones Científicas y Técnicas (CONICET- PIP 1122011010 0608) and Agencia Nacional de Promoción Científica y Tecnológica for financial support (PICT 1957 2012-PRESTAMO BID).

References

Ávila Ramírez, J. A., Juan Suriano, C., Cerrutti, P., & Foresti, M. L. (2014). Surface esterification of cellulose nanofibers by a simple organocatalytic methodology. *Carbohydrate Polymers*, *114*, 416–423.

Ávila Ramírez, J. A., Gómez Hoyos, C., Arroyo, S., Cerrutti, P., & Foresti, M. L. (2016). Naturally occurring α-hydroxy acids: Useful organocatalysts for the acetylation of cellulose nanofibres. *Current Organocatalysis*, *3*, 161–168.

Agustin, M. B., Nakatsubo, F., & Yano, H. (2016). The thermal stability of nanocellulose and its acetates with different degree of polymerization. *Cellulose*, *23*, 451–464.

Berlioz, S., Molina-Boisseau, S., Nishiyama, Y., & Heux, L. (2009). Gas-phase surface esterification of cellulose microfibrils and whiskers. *Biomacromolecules*, *10*, 2144–2151.

Blaker, J. J., Lee, K.-J., Walters, M., Drouet, M., & Bismarck, A. (2014). Aligned unidirectional PLA/bacterial cellulose nanocomposite fibre reinforced PDLLA composites. *Reactive & Functional Polymers*, *85*, 185–192.

Castro, C., Zuluaga, R., Putaux, J. L., Caroa, G., Mondragon, I., & Gañan, P. (2011). Structural characterization of bacterial cellulose produced by *Gluconacetobacter swingsii* sp. from Colombian agroindustrial wastes. *Carbohydrate Polymers*, *84*, 96–102.

Cerrutti, P., Roldán, P., Martínez García, R., Galvagno, M. A., Vázquez, A., & Foresti, M. L. (2016). Production of bacterial nanocellulose from wine industry residues: Importance of fermentation time on pellicles characteristics. *Journal of Applied Polymer Science*, *133*, 43109–43117.

Cunha, A. G., Zhou, Q., Larsson, P. T., & Berglund, L. A. (2014). Topochemical acetylation of cellulose nanopaper structures for biocomposites: Mechanisms for reduced water vapour sorption. *Cellulose*, *21*, 2773–2787.

De Marco Lima, G., Sierakowski, M.-R., Faria-Tischer, P. C. S., & Tischer, C. A. (2011). Characterisation of bacterial cellulose partly acetylated by dimethylacetamide/lithium chloride. *Materials Science and Engineering*, *31*, 190–197.

Domínguez de María, P. (2010). Minimal hydrolases: Organocatalytic ring-opening polymerizations catalyzed by naturally occurring carboxylic acids. *Chem-CatChem*, *2*, 487–492.

Foresti, M. L., Cerrutti, P., & Vazquez, A. (2015). Bacterial nanocellulose: Synthesis, properties and applications. In S. Mohanty, S. K. Nayak, B. S. Kaith, & S. Kalia (Eds.), *Polymer nanocomposites based on inorganic and organic nanomaterials* (pp. 39–61). Hoboken, NJ: John Wiley & Sons Inc.

Freire, C. S. R., Silvestre, A. J. D., Neto, C. P., Belgacem, M. N., & Gandini, A. (2006). Controlled heterogeneous modification of cellulose fibers with fatty acids: Effect of reaction conditions on the extent of esterification and fiber properties. *Journal of Applied Polymer Science*, *100*, 1093–1102.

Freire, C. S. R., Silvestre, A. J. D., Neto, C. P., Gandini, A., Martin, L., & Mondragon, I. (2008). Composites based on acylated cellulose fibers and low-density polyethylene: Effect of the fiber content, degree of substitution and fatty acid chain length on final properties. *Composites Science and Technology*, *68*, 3358–3364.

Gonçalves, S., Padra˜o, J., Rodrigues, I. P., Silva, J. P., Sencadas, V., Lanceros-Mendez, S., et al. (2015). Bacterial Cellulose as a support for the growth of retinal pigment epithelium. *Biomacromolecules*, *16*(4), 1341–1351.

Gonçalves, S., Padra˜o, J., Rodrigues, I. P., Silva, J. P., Sencadas, V., Lanceros-Mendez, S., et al. (2016). Acetylated bacterial cellulose coated with urinary bladder matrix as asubstrate for retinal pigment epithelium. *Colloids and Surfaces B: Biointerfaces*, *139*, 1–9.

Hafrén, J., & Córdova, A. (2005). Direct organocatalytic polymerization from cellulosefibers. *Macromolecular Rapid Communications*, *26*, 82–86.

Hestrin, S., & Schramm, M. (1954). Synthesis of cellulose by *Acetobacter xylinum:* 2. Preparation of freeze-dried cells capable of polymerizing glucose to cellulose. *Biochemical Journal*, *58*, 345–352.

Hu, W., Chen, S., Xu, Q., & Wang, H. (2011). Solvent-free acetylation of bacterial cellulose under moderate conditions. *Carbohydrate Polymers*, *83*, 1575–1581.

Ifuku, S., Nogi, M., Abe, K., Handa, K., Nakatsubo, F., & Yano, H. (2007). Surface modification of bacterial cellulose nanofibers for property enhancement of optically transparent composites: Dependence on acetyl-group DS. *Biomacromolecules*, *8*, 1973–1978.

Ilharco, L. M., Gracia, R. R., da Silva, J. L., & Ferreira, L. F. V. (1997). Infrared approach to the study of adsorption on cellulose: Influence of cellulose crystallinity on the adsorption of benzophenone. *Langmuir*, *13*, 4126–4132.

Jandura, P., Kokta, B. V., & Riedl, B. (2000). Fibrous long-chain organic acid cellulose esters and their characterization by diffuse reflectance FTIR spectroscopy, solid-state CP/MAS 13C-NMR, and X-ray diffraction. *Journal of Applied Polymer Science*, *78*, 1354–1365.

Johnson Ford, E. N., Mendon, S. K., Thames, S. F., & Rawlins, J. W. (2010). X-ray diffraction of cotton treated with neutralized vegetable oil-based macromolecular crosslinkers. *Journal of Engineered Fibers and Fabrics*, *5*, 10–20.

Kim, D., Nishiyama, Y., & Kuga, S. (2002). Surface acetylation of bacterial cellulose. *Cellulose*, *9*, 361–367.

Lee, K.-Y., & Bismarck, A. (2012). Susceptibility of never-dried and freeze-dried bacterial cellulose towards esterification with organic acid. *Cellulose*, *19*, 891–900.

Lee, K.-Y., Blaker, J. J., & Bismarck. (2009). Surface functionalisation of bacterial cellulose as the route to produce green polylactide nanocomposites with improved properties. *Composites Science and Technology*, *69*, 2724–2733.

Lee, K.-Y., Quero, F., Blaker, J. J., Hill, C. A. S., Eichhorn, S. J., & Bismarck, A. (2011). Surface only modification of bacterial cellulose nanofibers with organic acids. *Cellulose*, *18*, 595–605.

Missoum, K., Belgacem, M. N., & Bras, J. (2013). Nanofibrillated cellulose surface modification: A review. *Materials*, *6*, 1745–1766.

Segal, L., Creely, J. J., Martin, A. E., & Conrad, C. M. (1959). An empirical method for estimating the degree of crystallinity of native cellulose using the X-ray diffractometer. *Textile Research Journal*, *29*, 786–794.

Suetsugu, M., Kotera, M., & Nishino, T. (2009). Cellulosic nanocomposite prepared by acetylation of bacterial cellulose using supercritical carbon dioxide. In *17th international conference on composite materials*.

Tomé, L. C., Branda˜o, L., Mendes, A. M., Silvestre, A. J. D., Neto, C. P., Gandini, A., et al. (2010). Preparation and characterization of bacterial cellulose membranes with tailored surface and barrier properties. *Cellulose*, *17*, 1203–1211.

Tomé, L. C., Freire, M. G., Rebelo, L. P. N., Silvestre, A. J. D., Neto, C. P., Marrucho, I. M., et al. (2011a). Transparent bionanocomposites with improved properties prepared from acetylated bacterial cellulose and poly (lactic acid) through a simple approach. *Green Chemistry*, *13*, 419–427.

Tomé, L. C., Freire, M. G., Rebelo, L. P. N., Silvestre, A. J. D., Neto, C. P., Marrucho, I. M., et al. (2011b). Surface hydrophobization of bacterial and vegetable cellulose fibers using ionic liquids as solvent media and catalysts. *Green Chemistry*, *13*, 2464–2470.

Uschanov, P., Johansson, L.-S., Maunu, S. L., & Laine, J. (2011). Heterogeneous modi-fication of various celluloses with fatty acids. *Cellulose*, *18*, 393–404.

Yamamoto, H., Horii, F., & Hirai, A. (2006). Structural studies of bacterial cellulosetrough the solid-phase nitration and acetylation by CP/MAS ^{13}C NMR spectroscopy. *Cellulose*, *13*, 327–342.